Spreading of aqueous surfactant solutions on oil substrates

Kovalchuk, Nina M.; Sagisaka, Masanobu; Komiyama, Hinata; Simmons, Mark J. H.

DOI:
10.1016/j.jcis.2024.02.031

Document Version
Publisher's PDF, also known as Version of record

Citation for published version (Harvard):
Kovalchuk, NM, Sagisaka, M, Komiyama, H & Simmons, MJH 2024, 'Spreading of aqueous surfactant solutions on oil substrates: Superspreaders vs non-superspreaders', *Journal of Colloid and Interface Science*, vol. 661, pp. 1046-1059. https://doi.org/10.1016/j.jcis.2024.02.031

Journal of Colloid and Interface Science 661 (2024) 1046–1059

Contents lists available at ScienceDirect

Journal of Colloid And Interface Science

journal homepage: www.elsevier.com/locate/jcis

Regular Article

Spreading of aqueous surfactant solutions on oil substrates: Superspreaders vs non-superspreaders

Nina M. Kovalchuk [a,*], Masanobu Sagisaka [b], Hinata Komiyama [b], Mark J.H. Simmons [a]

[a] School of Chemical Engineering, University of Birmingham, B15 2TT, UK
[b] Graduate School of Science and Technology, Hirosaki University, 036-8561, Japan

GRAPHICAL ABSTRACT

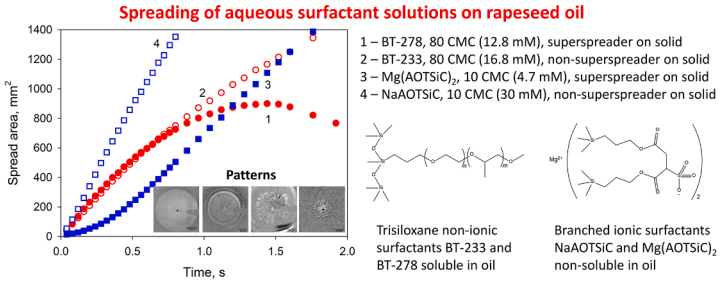

ARTICLE INFO

Keywords:
Branched ionic surfactants
Trisiloxane non-ionic surfactants
Mineral oil
Rapeseed oil
Superspreading
Interfacial tension
Spreading coefficient
Spreading exponent
Spreading patterns

ABSTRACT

Hypothesis: The question of why aqueous solutions of some surfactants demonstrate a rapid spreading (superspreading) over hydrophobic solid substrates, while solutions of other similar surfactants do not, has no definitive explanation despite numerous previous studies. The suggested hypothesis for this study assumes that once the spreading coefficient of surfactant is positive, there is a concentration range for solutions of any surfactant which demonstrates rapid spreading. As it is impossible to calculate spreading coefficients for solid substrates, we compare the spreading performance of known superspreaders and non-superspreaders on liquid (oil) substrate.
Experiments: The kinetics of spreading of aqueous solutions of a series of branched ionic surfactants and non-ionic trisiloxane surfactants on two liquid substrates was studied and compared with the spreading of a surfactant-free liquid, silicone oil. Both dynamic and equilibrium spreading coefficients were calculated using measured surface and interfacial tensions.
Findings: There is no difference in spreading rate on liquid substrate between solutions of surfactants proven as superspreaders (while spreading on solid substrate) or non-superspreaders. A rapid spreading (superspreading) with the characteristic rate of spreading O(10^2–10^3) mm^2/s occurs if the dynamic spreading coefficients exceeds the positive threshold value. If the dynamic spreading coefficient is negative or slightly positive, complete wetting still occurs, but the spreading is slow with the spreading rate is O(1) mm^2/s. Spreading exponents for surfactant solutions in the rapid spreading regime are considerably larger than for the surfactant-free liquid. A number of spreading and dewetting patterns were observed depending on the surfactant type, its concentration and substrate.

* Corresponding author.
E-mail address: n.kovalchuk@bham.ac.uk (N.M. Kovalchuk).

https://doi.org/10.1016/j.jcis.2024.02.031
Received 12 October 2023; Received in revised form 17 January 2024; Accepted 4 February 2024
Available online 6 February 2024

1. Introduction

The wetting and spreading of liquids onto both solid and liquid substrates is of great importance for many applications: painting and coating, enhanced oil recovery, firefighting (aqueous film forming foams), agriculture (application of foliar fertilisers and pesticides), medicine (application of lung or dry eyes medications) to name a few, see [1] and references herein. All of these listed applications rely on complete wetting and fast spreading. This task becomes especially challenging when the spreading formulation is aqueous and substrate to be wetted is hydrophobic. In many cases, this problem can be solved by adding a surfactant or surfactant mixture to the formulation.

The most commonly known spreading promoters for hydrophobic solids are trisiloxane surfactants called superspreaders [1–4] which enable spreading of aqueous formulation into a thin film, several micrometres in thickness, within seconds or tens of seconds depending upon the initial drop size. Some ionic surfactants with a highly branched structure [5] and mixtures of cationic and anionic surfactants [6] demonstrate a similar performance.

The wetting status of a drop placed on a substrate/air interface is determined by the spreading coefficient [7]

$$S = \sigma_{SA} - (\sigma_{SL} + \sigma_{LA}) \tag{1}$$

where σ_{SA}, σ_{SL} and σ_{LA} are interfacial tensions at substrate/air, substrate/liquid and liquid/air interface accordingly. In the case of spreading on substrate/liquid interface, air should be replaced by the second liquid. Eq. (1) can be also considered as the energy balance related to spreading if σ_{SA}, σ_{SL} and σ_{LA} are considered as specific surface energies. Complete wetting is energetically favourable only if sum of energies of newly created substrate/liquid and liquid/air interfaces is smaller than the initial energy of substrate in contact with air. A value of $S > 0$ is therefore the necessary condition for complete wetting, but the question remains unanswered as to whether a positive value of spreading coefficient is a sufficient condition for superspreading and the mechanism of superspreading is still under debate. One of the reasons for this is that superspreading is usually related to solid substrates. For these, values of σ_{SA} can be estimated from a series of wetting experiments [8,9], although with rather large uncertainty [10]. For the case of partial wetting, σ_{SL} can be found from the Young's equation (2), but it is impossible to find σ_{SL} for the case of complete wetting and, therefore, the value of the spreading coefficient is always unknown on solid substrate.

Spreading on a liquid substrate overcomes this difficulty, because all interfacial tensions included in Eq. (1) can be measured. Moreover, the liquid substrate is molecularly smooth enabling all issues related to substrate structure and roughness to be discarded, including wetting state, Wenzel or Cassie-Baxter [11,12]. There are, however, some essential differences in spreading conditions on solid and liquid substrates which make it difficult to translate directly the results obtained from a liquid substrate to spreading on a solid substrate. Firstly, no-slip boundary conditions apply to the solid/liquid, but not to the liquid/liquid interface. From theoretical point of view that means that the spreading on liquid can be modelled and analysed easier than that on solid, where there is violation of the no-slip boundary conditions at three phase contact line (TPCL). The practical implication of this difference is faster spreading on a liquid than that on a solid substrate. The number of parameters affecting spreading kinetics on liquid increases, adding to the list the substrate viscosity and its depth.

In the case of partial wetting, the substrate/liquid interface remains non-deformable if the substrate is solid and a single equilibrium macroscopic contact angle can be found from Young's equation [7]

$$cos\theta = \frac{\sigma_{SA} - \sigma_{SL}}{\sigma_{LA}} \tag{2}$$

although for most substrates there exists a noticeable difference between the advancing and receding contact angle.

A liquid substrate is deformable, therefore the wetting liquid forms a lens, as shown in Fig. 1, for the simplest case when gravity is neglected and the substrate/air interface in the vicinity of liquid lens is not deformed. There are now two independent contact angles, γ and β related to the lens/air and lens/substrate interface. The contact angles can be found from tangential and normal balance of interfacial stresses at TPCL forming the Neumann triangle, see [13,14] and references herein

$$cos\theta_1 = \frac{\sigma_{LA}^2 - \sigma_{SA}^2 - \sigma_{SL}^2}{2\sigma_{SA}\sigma_{SL}} \tag{3a}$$

$$cos\theta_2 = \frac{\sigma_{SA}^2 - \sigma_{LA}^2 - \sigma_{SL}^2}{2\sigma_{LA}\sigma_{SL}} \tag{3b}$$

$$cos\theta_3 = \frac{\sigma_{SL}^2 - \sigma_{SA}^2 - \sigma_{LA}^2}{2\sigma_{SA}\sigma_{LA}} \tag{3c}$$

From geometrical considerations $\gamma = 180^\circ - \theta_3$, $\beta = 180^\circ - \theta_1$, $\gamma + \beta = \theta_2$.

Note, in the case of complete wetting both γ and β →0 and Eq. (1) still holds as a condition for the complete wetting of liquid substrate.

Another essential difference between wetting on a solid and liquid substrate is the structure of the adsorption layer at the substrate/liquid interface. For a liquid/liquid interface, similar to a liquid/air interface, the adsorption layer is usually uniform except for the rare cases of soluble surfactants where domains of liquid-condensed phase are formed [15]. At the same time, formation of self-assembled structures at the liquid/solid interface is more common. It is essential for spreading, that the shape of these structures resembles the structure of bulk aggregates. It was observed using atomic force microscopy (AFM) that micellar solutions of tetradecyl trimethylammonium bromide (C_{14}TAB) form cylindrical aggregates on the surface of hydrophobic graphite [16]. The same curved shape of aggregates, but more resembling worm like micelles was observed also on hydrophilic mica [16]. A similar aggregate shape was observed in the adsorption layer of hexadecyltrimethylammonium bromide (C_{16}TAB) on mica in [17] where it was assumed that, in this case, a bilayer structure was formed with the flat layer adjacent to the solid surface with cylindrical micelles on the top of

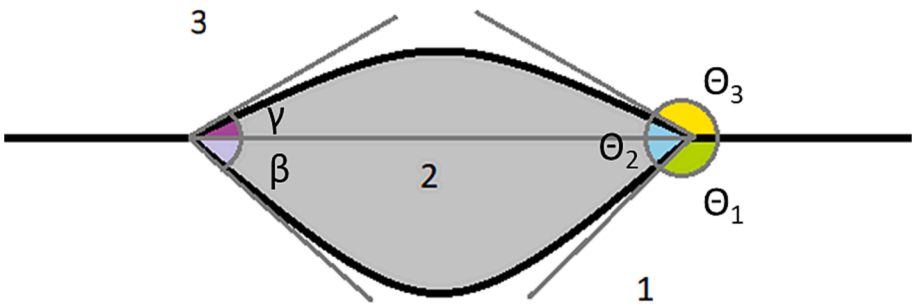

Fig. 1. Neumann triangle for partial wetting at liquid/liquid interface.

it. It is interesting to note that the addition of gemini surfactant, 1,2-bis (dodecyldimethylammonio)ethane dibromide, to the solution resulted in a transition from cylindrical micelles to a flat bilayer [17].

It was suggested in [4] that the difference in the aggregate structure on the solid interface affects the value of σ_{SL}, with cylindrical aggregates leading to higher values of interfacial tension and therefore a smaller spreading coefficient. This explains why two surfactants can have the same surface tension, but the only the one forming bi-layer aggregates in the bulk demonstrates superspreading: for micellar surfactant σ_{SL} can be too large, leading to negative spreading coefficient. This suggestion is in agreement with results presented in [18] for adsorption of a superspreading trisiloxane surfactant on graphite. For this surfactant, superspreading begins at a critical wetting concentration (CWC) which is noticeably higher than the CMC. The AFM study in [18] has shown the formation of strip-like structures on the substrate, indicating formation of cylindrical aggregates at a concentration CMC < C < CWC, whereas for C > CWC, AFM shows a featureless structure, characteristic of a lamellar bi-layer. Therefore, one of the points of interest of studying spreading on a liquid substrate is comparison of the spreading coefficients obtained for known superspreading and non-superspreading surfactants, and their spreading kinetics on liquid substrate.

For the case of compete wetting, it is generally accepted that surfactant solutions, in particular superspreaders, spread considerably faster than pure liquids on a solid substrate. Surprisingly, the converse is true for spreading on a liquid substrate, where it is suggested that surfactant solutions spread at the same rate or even more slowly than the pure liquid. The main reason for this difference is the basis of comparison: for spreading on a solid substrate, the comparison is made for the movement of TPCL of macroscopic drop on both substrates, whereas for a liquid substrate, the rate of propagation of the precursor film for a pure liquid is compared with the rate of propagation of the TPCL of the macroscopic drop of surfactant solution.

There is also a striking difference in the approaches taken in identifying the governing parameters of importance in the spreading mechanisms on solid and liquid substrates. Numerical simulations [19,20] have shown that considerable acceleration of the spreading on a solid can be achieved in the presence of Marangoni stresses in the direction of the TPCL. In the case of a cylindrical (2D) drop, where the spread area is proportional to the radius of spreading, R, advection of surfactant results in surfactant accumulation near the TPCL and slows down the spreading. Superspreading was achieved in these simulations only if the adsorption of surfactant onto the solid through the TPCL enabled establishment of the Marangoni stresses in the right direction. It was shown in [20], that there is an optimal range of the surfactant leakage from liquid/air interface through the TPCL to enable superspreading. In most experiments, the spread area is circular, i.e. $\sim R^2$. Therefore, it was suggested that depletion of surfactant in the vicinity of the TPCL due to the considerable increase of surface area, can overpower the advection and facilitate formation of surface tension gradients accelerating spreading [3]. Despite above mentioned results the relative importance of surface tension gradients on the spreading kinetics on solids is still debatable [4], whilst Marangoni stresses are considered as the main mechanism of spreading on liquid substrates. It is worthy of mention that formation of surface tension gradients is sensitive to the initial conditions. Simulations of spreading of surfactant solutions on a liquid interface using the same approach as in [19], but under the condition of zero initial adsorption (surfactant is present only in the bulk at t = 0), show reduced concentration of surfactant near the TPCL during spreading [21].

The generally accepted model for spreading of a surfactant-free liquid over a solid substrate is the Tanner model, based on the balance between capillary and viscous forces which predicts the spreading kinetics as [22]

$$A \sim \left(\frac{\sigma_{LA} V^3}{\mu}\right)^{0.2} t^{0.2} \tag{4}$$

where A is the spread area, V is the drop volume, μ is the dynamic viscosity of spreading liquid and t is the time. Numerous experimental studies, mostly using silicone oil as a spreading liquid, have confirmed the validity of this model, with the spread area increasing in proportion to $t^{0.2}$. The exponent on t is the spreading exponent, denoted α. Note, according to Eq. (4), the spreading kinetics is independent of the spreading coefficient. It is generally accepted that spreading of pure liquid on a solid is accompanied by formation of a very thin precursor film in front of the spreading main drop. Therefore, all chemical energy related to the positive spreading coefficient is consumed by the precursor film. The macroscopic drop is considered to be in contact with the precursor film made of the same material, which makes the spreading coefficient at the contact line between the macroscopic drop and the film close to zero [23,24]. Eq. (4) is not applicable to spreading of the precursor film which is dependent on spreading coefficient.

Eq. (4) was derived under the condition when drop size is smaller than the capillary length $L_c = \sqrt{\frac{\sigma_{LA}}{\rho g}}$ (ρ is the liquid density, g is acceleration due to gravity). In this case, the effect of gravity is negligible. In the opposite case, when the gravity is the main driving force, the spreading exponent increases to 0.25 with [25]

$$A \sim \left(\frac{\rho g V^3}{\mu}\right)^{0.25} t^{0.25} \tag{5}$$

When the drop size is O(L_c) the gradual transition from kinetics of Eq. (4) to that of Eq. (5) was observed [26].

Comparison of the spreading kinetics of surfactant-free liquids and superspreading surfactant solutions on solid substrates shows that surfactant solutions spread much faster with the spread area being proportional to time. According to [27], the spread area of a 5 mL drop of a superspreading trisiloxane solution at t = 14 s was 4 times larger than the spread area of a 1 mPa s viscosity silicone oil drop of the same volume. It should be noted, however, that Eq. (4) is probably not applicable for the case of aqueous surfactant solutions spreading over the solid hydrophobic substrate, because the presence of liquid film spreading fast in the front of the main drop is questionable. There are suggestions about surfactant molecules being adsorbed in the front of the TPCL and facilitating spreading [28]. Moreover, formation of a bilayer precursor film with A ~ t was confirmed by spreading of pure (without water added) trisiloxane superspreader [29]. However, kinetics of this precursor spreading was too slow, O(0.1) mm^2/hour, to account for the fast superspreading of aqueous solutions.

In contrast with a solid substrate, where the presence and spreading kinetics of the precursor film is difficult to estimate experimentally, this is a relatively simple task for spreading on liquid interface, where it is easily followed by seeding the surface of the substrate with small O(1) μm neutrally buoyant particles. For example, it was observed in [23] that for the spreading of silicone oil on an aqueous substrate, the particles started moving long before the macroscopic TPCL reached them, confirming spreading of a precursor film. The spreading kinetics of the precursor film was estimated in [23] as A ~ t. As a consequence of such observations, the modelling of spreading kinetics on liquid substrates has mostly focused on the spreading of precursor film.

The model was initially developed for spreading of an insoluble surfactant monolayer over the liquid surface, an example being the spreading of oleic acid over an aqueous subphase. In this case the main driving force for spreading is the surface tension gradient between the surfactant-laden and the surfactant-free surface. An analogue for spreading coefficient can be introduced as $S = \sigma_0 - \sigma_{min}$, where σ_0 is the surface tension of the clean substrate and σ_{min} is the surface tension of the substrate when fully covered by surfactant. It is noticeable that the kinetics for both monolayer and precursor film spreading are the same, the difference is only in the definition of S. The simple scaling estimation for monolayer spreading kinetics on a thin liquid substrate gives [30]

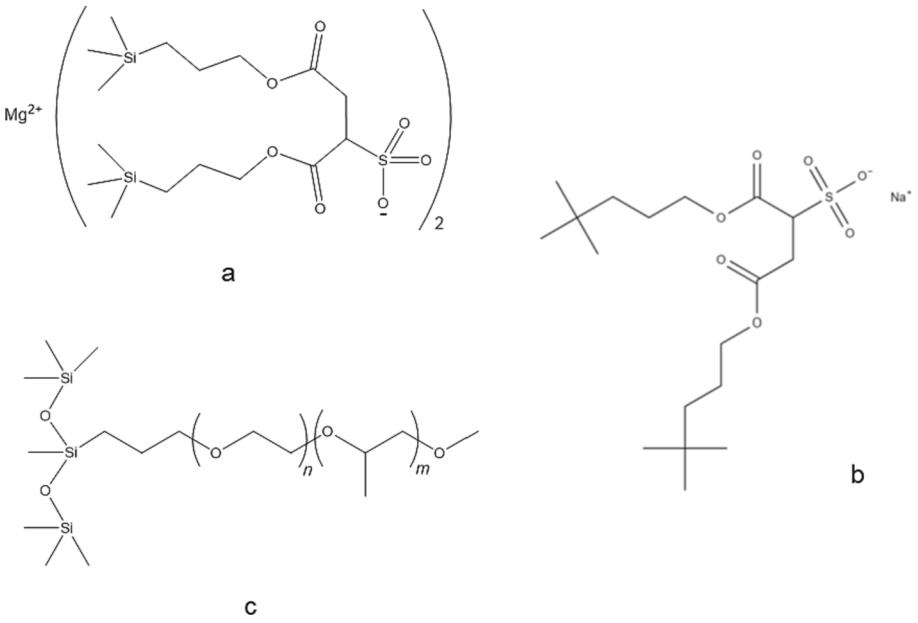

Fig. 2. Structure of surfactants used in the study: a – $Mg(AOTSiC)_2$, b – NaAOTtBC, c – generalised structure of trisiloxane surfactant.

$$A = K_1 \frac{HS}{\mu_s} t \tag{6}$$

where H is the substrate thickness, μ_S is substrate viscosity and K_1 is a coefficient of O(1). A similar scaling for a precursor film was derived in [23].

For spreading over a deep liquid layer, the substrate effect on the spreading kinetics is determined by the hydrodynamic penetration depth on the time scale of spreading and spreading kinetics is given by

$$A = K_2 \frac{S}{(\mu_s \rho_s)^{0.5}} t^{1.5} \tag{7}$$

where K_2 is a coefficient of O(1) and ρ_s is the density of substrate liquid. Eq. (7) is valid for spreading of a surfactant monolayer as well as for spreading of precursor films, see [31–33] and references herein. The kinetics of liquid film spreading on a liquid substrate according to Eq. (7) was confirmed in multiple experiments including spreading of oil on aqueous surfactant solutions [32].

To describe the spreading of the main drop in contact with precursor film on a thin liquid substrate, an approach similar to spreading on a solid was applied in [23], using the lubrication approximation, where the thickness of substrate is much smaller than the radius of spreading, and the thickness of spreading drop is much smaller than the thickness of substrate. According to [23], for capillary pressure driven spreading $A \sim t^{1/4}$, whereas for gravity driven spreading $A \sim t^{1/3}$. It was however noted in [23] that from experiments, the spreading exponent depends on the definition of drop boundary and varies in the range 0.3 – 0.9 with larger exponents found closer to the precursor film.

If the viscosity of a spreading drop is considerably higher than the substrate viscosity, then the spread area depends on drop viscosity instead of substrate viscosity provided that the condition $\mu > \mu_s \frac{R}{h}$, with h being the lens height, is fulfilled. The spread area changes with time as [34]

$$A = 4\left(\frac{\pi V \sigma_{LA}}{\mu}\right)^{0.5} t^{0.5} \tag{8}$$

with spreading on a liquid being considerably faster than spreading on a solid, Eq. (4), as expected.

Note that spreading on a solid accelerates if the substrate is considered as slippery. It was demonstrated in [35] that provided that the drop height, h, is much larger than the slip length, λ, the spreading follows Eq. (4), but when $h < \lambda$

$$A\ \pi\left(\frac{V^2 \lambda \sigma_{LA}}{\mu}\right)^{0.25} t^{0.25} \tag{9}$$

For low molecular weight liquids, such as water and aqueous solutions of surfactants considered in the present study, the slip length is of order of 1 nm and therefore this regime cannot be observed, but for some high molecular mass polymers, λ can reach 10 μm and the strong slip regime becomes realistic, see [35] and references herein. However, comparison between Eq. (8) and Eq. (9) shows that even in the presence of a strong slip the kinetics of spreading on a solid are slower than that on a liquid.

The spreading of a surfactant solution over a liquid substrate in the case of complete wetting is not accompanied by the formation of a precursor film [33], which supports the suggestion that there is no such film accompanying spreading on a solid substrate. It was shown in [33] that the spreading of a thin lens should follow the same kinetics as the precursor film if it is driven by Marangoni stresses (spreading coefficient). Although the interest in spreading of aqueous formulations over liquid hydrocarbon substrates is growing, especially in relation to aqueous fire-fighting foams, both experimental and numerical studies are still rather scarce [21,33,36–41]. The general conclusion from these studies is that the spreading kinetics is limited by the surfactant adsorption kinetics as well as by the dissolution of surfactant in substrate phase. The kinetics get closer to the predictions of Eq. (7) at large surfactant concentrations, enabling fast surfactant equilibration which replenishes surfactant depleted at the expanding liquid/liquid and liquid/air interface [21,33,36,37]. It was suggested in [33] that for the fastest spreading, the surface/interfacial tension at liquid/air and liquid/substrate interface at the centre of spreading drop should be at their minimum, corresponding to equilibrium values at CMC. A positive spreading coefficient close to zero should be maintained at TPCL. This will create the maximum surface tension gradient between the central part of the drop and TPCL accelerating spreading, while still making spreading thermodynamically favourable ($S > 0$). It is possible that the same mechanism can work for spreading over a solid substrate and contribute to setting the caterpillar motion (rolling) at TPL considered as an important feature of superspreading on solid substrate [4,42].

In summary, there are a limited number of studies on the spreading of aqueous surfactant solutions over liquid hydrocarbon substrates with limited choice of surfactants. To the authors' best knowledge, there are

Table 1
Surfactant properties.

	NaAOTtBC	$Mg(AOTtBC)_2$	NaAOTSic	$Mg(AOTSiC)_2$	BT-278 [44]	BT-233 [44]
Molar mass, g/mol	416	810.3	448.7	875.7	625	857
CMC, mM	4.44	1.99	3.0	0.47	0.16	0.21
Surface tension at CMC, mN/m	23.3	22.5	22.8	21.8	21.7	23.6

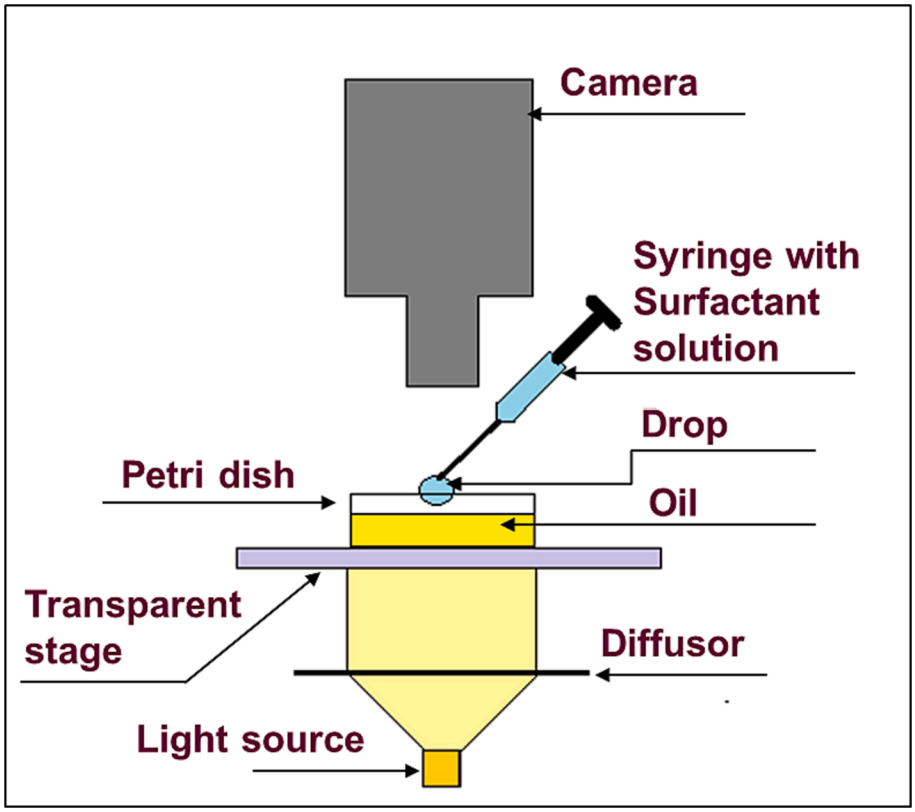

Fig. 3. Experimental set up for study of spreading of aqueous surfactant solutions on oil substrate.

no studies comparing kinetics at the TPCL of a macroscopic drop for surfactant-free liquid and surfactant solution or comparison of the spreading performance of surfactant solutions on liquid substrates which demonstrate either superspreading or non-superspreading on solid substrates. The aim of this study is thus to fill this gap and compare the kinetics of spreading of the main drop of surfactant-free liquid on liquid substrate with spreading kinetics of surfactant solutions on substrates of similar viscosities to examine the possible similarity/dissimilarity with spreading on a solid substrate. Unlike previous studies, we compare the spreading kinetics for different types of surfactants: ionic and non-ionic, i.e. both soluble and insoluble in the substrate phase, those demonstrating superspreading and non-superspreading behaviour on solids, surfactants forming micelles, bi-layer type of self-assembled structures and those forming sediments above the solubility limits.

An additional aim of this study is to probe the spreading performance of solutions of novel branched ionic surfactants with low surface tension. Effective ionic surfactants are important for spreading over liquid oil substrates, as well as for spreading over solid substrates in contact with oil, because as a rule they are insoluble in the oil phase and therefore more effective for such applications.

2. Materials and methods

The ionic branched surfactants, sodium salt of bis (3-(trimethylsilyl)-propyl) 2-sulfosuccinate, NaAOTSiC; magnesium salt of bis (3-(trimethylsilyl)-propyl) 2-sulfosuccinate, $Mg(AOTSiC)_2$; sodium bis (*t*-butyl propylene) 2-sulfosuccinate, NaAOTtBC; magnesium di (*t*-butyl propylene) 2-sulfosuccinate), $Mg(AOTtBC)_2$ were synthesised following the procedure described in the Supporting information (SI-1) for NaAOTtBC and $Mg(AOTtBC)_2$, in [43] for NaAOTSiC and in [5] for NaAOTSiC and $Mg(AOTSiC)_2$. $Mg(AOTSiC)_2$ has been proven as superspreader, providing similar kinetics to trisiloxane superspreaders on a hydrophobic solid substrate of polyvinylidenefluoride [5]. All other ionic surfactants in this study did not demonstrate superspreading on this solid substrate. The non-ionic trisiloxane superspreader BREAK-THRU S 278, BT-278, and non-superspreading trisiloxane surfactant BREAK-THRU S 233, BT-233, were supplied as a gift from Dr Joachim Venzmer (Evonic). Ionic surfactants are practically insoluble in the substrate oils, whereas non-ionic surfactants are soluble. The structures of the surfactants are presented in Fig. 2 and their properties at room temperature are presented in Table 1. All aqueous solutions were prepared using double-distilled water produced by an Aquatron A 4000 D water still (Stuart).

Solutions of NaAOTSiC and NaAOTtBC at concentration of 1.25 times the CMC were visually transparent, but become translucent with a further increase of concentration, indicating transition from micellar to bi-layer forming solutions. Indeed, SANS data for NaAOTSiC (see Fig. S1 and Table S1 in the Supporting Information) indicate the presence of nearly spherical micelles at a concentration of 2 CMC, but ellipsoidal micelles and bi-layer structures form at 10 CMC. It is well-known from

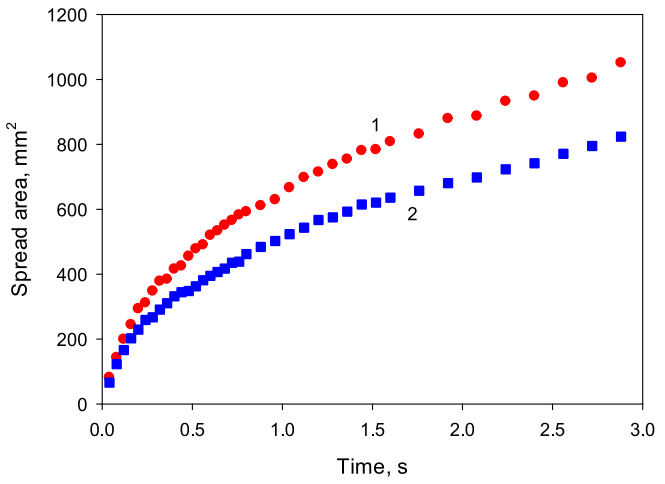

Fig. 4. Spreading kinetics of silicone oil on 80:20 glycerol/water mixture (1) and 85:15 glycerol/water mixture (2).

the literature that solutions of BT-278 self-assemble in bi-layer type aggregates at concentrations above the CMC, whereas solutions of BT-233 form micelles [45].

For solutions of $Mg(AOTtBC)_2$ and $Mg(AOTSiC)_2$, the values of CMC provided in Table 1 most probably correspond to solubility limits. Solutions at 1.25 CMC are nearly transparent, but those at higher concentrations are milky and after some time sediment starts to form at the bottom of the flask. To prevent sedimentation on the time scale of the spreading experiments, solutions (dispersions) were subjected to multiple cycles of alternated vibro-mixing/ultrasonicating and filtered through 1 μm syringe filter immediately before use. It was impossible to control the exact amount of solid retained within the filter. Therefore, the concentrations used below are concentrations before filtering and the actual concentrations of surfactant used are smaller.

Mineral oil, MO, (Sigma M5904) with density 845 kg/m^3, viscosity 31 mPa s and surface tension 31.7 mN/m and vegetable (rapeseed) oil, VO, (Sainsbury's) with density 918 kg/m^3, viscosity 70 mPa•s and surface tension 34.5 mN/m, were used as liquid substrates. For comparison, silicone oil 5 cSt (Sigma) of viscosity 4.6 mPa s and surface tension 19 mN/m was spread on substrates of 80:20 and 85:15 glycerol/water mixtures by mass matching the kinematic viscosity of mineral and rapeseed oil at room temperature respectively [46]. The surface tension of water/glycerol mixtures was 65 mN/m and interfacial tension between silicone oil and glycerol/water mixtures was 32 mN/m. Glycerol, ultrapure, HPLC grade, was purchased from Alfa Aesar.

Densities were measured using glass pycnometer with volume of 25.877 cm^3. Viscosities were measured by a Discovery-HR-2 rheometer (TA instruments) using cone and plate geometry with the angle of 2° 00′ 292 and a truncation of 55 μm. The interfacial tension between the aqueous solution and oil and dynamic surface tension of aqueous solutions was measured with a PAT1 tensiometer (Sinterface) using drop profile analysis. Equilibrium surface tension of aqueous solutions was measured using a CBVP-Z tensiometer (Kyowa Interface Science) equipped with a platinum Wilhelmy plate.

The experimental set up is presented in Fig. 3. For the spreading experiment, 25 mL of substrate was poured into glass Petri dish (inner diameter 70 mm) using a 5 mL Eppendorf pipette. The thickness of oil layer was approximately 6.5 mm, being large enough to eliminate the influence of the solid bottom of the Petri dish upon the wetting dynamics [33]. The Petri dish was set on a transparent horizontal stage and illuminated from below by a cold light source KL 2500 LED (SCHOTT).

A 1 mL syringe (BD Plastipak) was filled with the spreading liquid and placed into a micrometer syringe outfit AGLA (Burroughs Wellcome & Co, UK). The syringe was equipped with a stainless-steel needle 30 GA (0.159 mm ID, 0.312 mm OD) ½" (METCAL). The angle between the syringe and oil surface was approximately 45° to fit into the space between the surface and the camera lens. A drop of spreading solution was formed manually at the tip of the needle using a micrometric screw to gradually move the syringe plunger. The drop detached from the needle due to gravity at a height of around 1 mm from the oil surface. The average drop volume was 4.0 ± 0.3 mm^3, based on weighing 100 drops. The drop radius is smaller than the capillary length, therefore the effect of gravity is negligible and the drop is small enough to float on the substrate surface despite its larger density [47].

Drop spreading was recorded by high speed video camera SA3 (Photron) equipped with a 24–85 mm lens AF NIKON at 125 fps, exposure time 0.5 ms, field of view 1024 × 1024 pixel^2 and spatial resolution 50 μm/pixel. For NaAOTtBC 1.25CMC, due to small spread area, spreading was recorded using camera connected to an inverted optical microscope Nikon Ti-U equipped with 4 × lens providing resolution 5 μm/pixel. Image processing was carried out using ImageJ [48]. The spreading exponents were found by carrying out a linear fitting to the data of the spread area vs time dependence on log–log scale. Some graphs demonstrated several stages of spreading with different slopes (spreading exponents). In this case the exponent for the highest spreading rate was reported in Figures.

All experiments were carried out at least in triplicate at room temperature 22 ± 2 °C. The humidity was not controlled, but was measured, enabling series of experiments for surfactant solutions to be performed at low and high room humidity in the range of RH 24 – 55 %.

3. Results and discussion

The spreading coefficient for silicone oil on both aqueous substrates is around 14 mN/m. The values of surface/interfacial tension for all studied surfactant solutions and calculated values of spreading coefficients on both oil substrates are given in Table 2, see Appendix, where the numerator corresponds to the dynamic surface/interfacial tension at the beginning of measurement (estimated time of 3–5 s for drop profile instruments), whereas the values in the denominator correspond to equilibrium surface/interfacial tension. It is seen from Table 2, that for the most of surfactant solutions, the dynamic surface/interfacial tension is rather close to if not the same as the equilibrium value. The exception is only the smallest concentration of sodium surfactants. The dynamic interfacial tension at water/oil interface for these surfactant solutions is shown in Fig. S2a and dynamic surface tension (water/air interface) is presented in Fig. S2b. Table 2 shows that interfacial tension of the solutions of trimethylsilyl ionic surfactants is considerably lower than that of solutions of hydrocarbon ionic surfactants, due to higher hydrophobicity of trimethylsilyl group [49]. All spreading coefficients for surfactant solutions are smaller than the spreading coefficient of silicone oil on aqueous subphase.

3.1. Spreading of silicone oil on aqueous substrates

Snapshots of spreading silicone oil on aqueous phase are presented in Fig. S3. They display ridge formation at the leading edge of spreading. The spread area was measured for the 3 first seconds of spreading. A precise enough measurement at later times was impossible due to relatively low contrast. Kinetics of spreading is presented in Fig. 4. As expected, spreading is slower on higher viscosity subphase. Spreading exponents of $\alpha = 0.49 \pm 0.01$ for substrate of 85:15 glycerol/water mixture and $\alpha = 0.48 \pm 0.01$ for substrate of 80:20 glycerol/water mixture were the same for the whole observation time and are in good agreement with experimental data reported in [23] for spreading on the thin liquid layer. The crossover between a thin and a deep liquid layer is determined by the hydrodynamic penetration depth, $\sqrt{\mu t/\rho}$ at time scale of spreading [37]. Considering that the time scale of spreading experiments in this study is 1 – 4 s, the cross-over depth is in the range of 6 – 17 mm, i.e. our substrate can be considered as the top margin of the thin

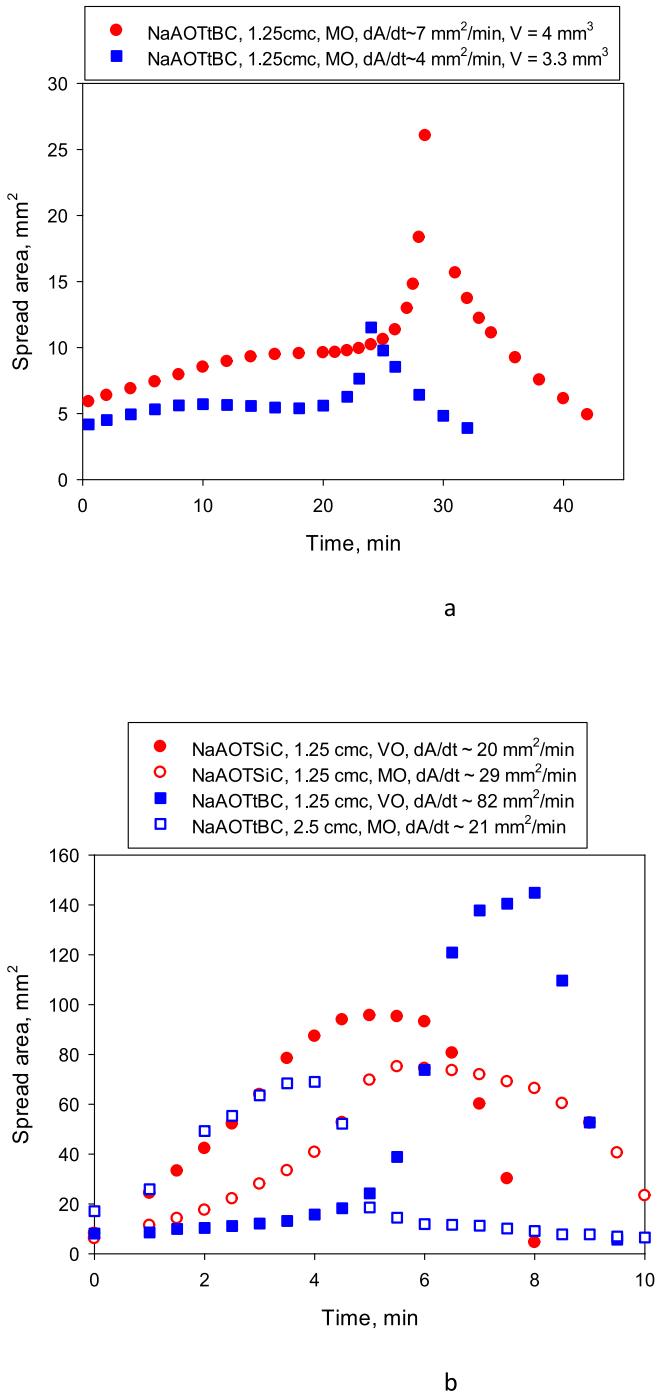

Fig. 5. Spreading kinetics of Na surfactants at small spreading coefficients, MO = mineral oil, VO = rapeseed oil.

substrate. It should be stressed that the kinetics are much slower than predicted and observed in experiments for a precursor film on both thin and deep substrate.

3.2. Slow spreading of ionic surfactant solutions with negative or small positive dynamic spreading coefficient

In spreading experiments for surfactant solutions on oil, the drop formation before deposition on the substrate takes around 10–15 s; at that time scale, the spreading coefficient for both 1.25 CMC Na surfactant solutions on both oils was negative. Therefore, for these surfactant solutions, the drop formed a lens on the oil immediately after deposition. The two following processes then took place: surfactant adsorption at oil/water and water/air interface and drop evaporation. Evaporation at room temperature is rather slow process. A 4 mm^3 drop of water placed on mineral oil evaporates completely within around 3 h at a temperature of 22 °C and a relative humidity of 54 %. The water evaporation should be faster for surfactant solutions because the rate of evaporation is proportional to the lens size [50].

It was possible to follow the lens kinetics during the whole process up to full evaporation of water with high spatial resolution for a solution of 1.25 CMC of NaAOTtBC on mineral oil for slightly smaller drop of 3.3 mm^3 in volume owing to its small maximum spread area enabling microscopic observation. For the drop of 4 mm^3, the maximum spread area was slightly larger than the field of view and was found as an intersection of ascending and descending branches. The results for both drop sizes are presented in Fig. 5a. The data for this composition is presented in a separate graph, because for the time scale of spreading is considerably larger in this case, whereas the maximum spread area is considerably smaller than for other solutions demonstrating the slow spreading. At drop deposition, the estimated spreading coefficient is around −7.1 mN/m and drop forms a lens with $\gamma = 15.3°$ and $\beta = 73.5°$. Due to much smaller interfacial tension at the water/oil interface than at the water/air interface $\gamma \ll \beta$, the lens is asymmetrical with respect to the oil surface, with most of the lens being situated inside the oil phase. Considering that the drop density was larger than the substrate density, gravity can also contribute to this asymmetry. The asymmetry was clearly observed from the side view of the lens.

After deposition, the lens cross-sectional area gradually increases as surfactant adsorbs at substrate/ liquid and liquid/air interface and both surface and interfacial tension decrease. An increase in the lens size intensifies evaporation and after certain time a decrease in the lens area due to evaporation becomes comparable with its increase due to spreading, i.e. evaporation leads to a slowing of spreading. For the smaller drop there was even some decrease of the drop cross-section. Such a decrease does not contradict the physics of continuing surfactant adsorption and the corresponding decrease of contact angle, because the volume of drop decreases due to evaporation. The last causes an increase of the bulk surfactant concentration and further increase of surfactant transfer to the interface. As a result, the spreading coefficient becomes positive, causing transition to a regime of complete wetting and an acceleration of spreading. Transition from partial to complete wetting is seen in drop images, where fast spreading coincides with the abrupt decrease in the image contrast due to lens curvature going to zero as shown in Fig. S4. After several minutes of the spreading, the spread area decreases rapidly, most probably due to further evaporation. The drop retains small surface curvature as seen from comparison of Fig. S4, 36 min and Fig. S4, 2 min.

Notably, after the area of spread film was reduced to around 4–5 mm^2, it started to oscillate as shown in video S1. After each oscillation the area of the film decreased noticeably until it disappeared completely. As the whole process is governed to the large extent by evaporation it depends considerably on the ambient temperature and humidity. Considering that surfactant is not volatile and not soluble in the oil phase, drop disappearance due to evaporation should mean formation of a thin liquid film (Newton or common black film [51]) stabilised by surfactant adsorbed on both water/oil and water/air interfaces.

An increase in concentration of NaAOTtBC to 2.5 CMC leads to a small positive value of spreading coefficient on mineral oil and spreading under condition of complete wetting begins immediately after drop deposition (Fig. 5b). The spreading coefficient of 1.25 CMC of NaAOTtBC on rapeseed oil is initially negative and it takes more than 4 min for the deposited drop to reach condition for complete wetting, but spreading is fastest among the cases presented in Fig. 5b and thus the spread area is largest.

For NaAOTSiC solutions, the surface/interfacial tension decreases relatively quickly and spreading coefficient becomes positive after 30 s

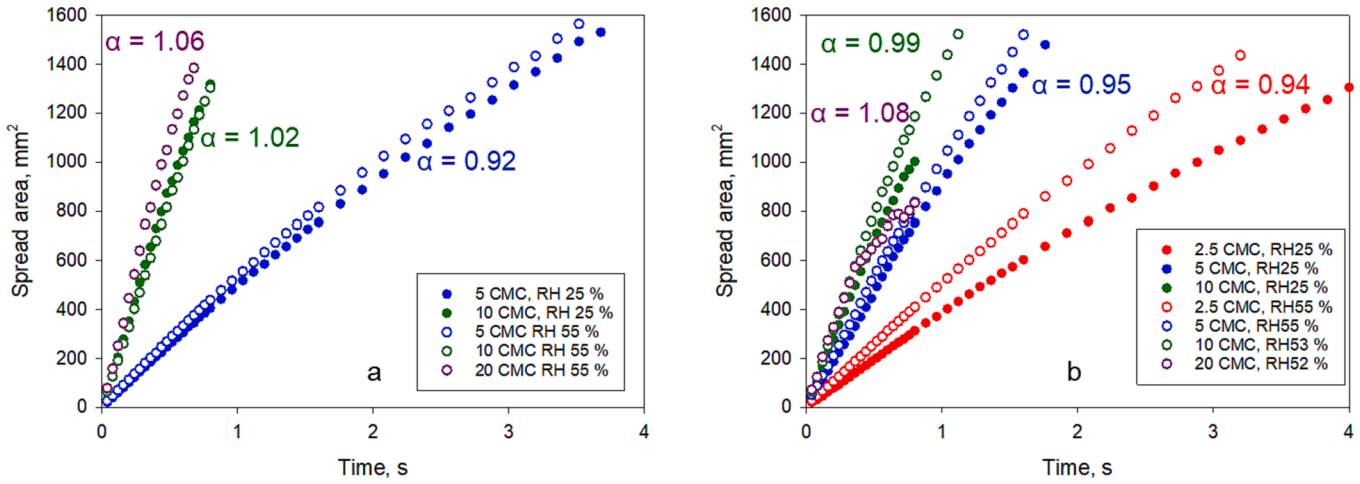

Fig. 6. Spreading kinetics of NaAOTtBC on mineral oil (a) and rapeseed oil (b). The spreading coefficients on mineral oil (a) are: 5 CMC – 5.9 mN/m, 10 CMC – 7.7 mN/m, 20 CMC – 8.4 mN/m. The spreading coefficients on rapeseed oil (b) are: 2.5 CMC – 4.4/7.4 mN/m, 5 CMC – 6.5/8.4 mN/m, 10 CMC – 10.0 mN/m, 20 CMC – 10.7 mN/m.

for spreading on rapeseed oil and after 2 min for spreading on mineral oil. Similar to NaAOTtBC, spreading on rapeseed oil is faster than on mineral oil and the final spread area is larger. In general, for all cases where the initial spreading coefficient is negative or positive but rather small, spreading process in the regime of complete wetting is very slow, on the time scales of minutes, i.e. much slower than that of silicone oil on aqueous substrate. Note, for the initially negative spreading coefficient, complete wetting starts after some induction period when the spreading coefficient becomes positive due to increase of dynamic surface/interfacial tension. The maximum spreading rate is in the range 0.12 – 1.4 mm^2/s. Transition from the lens to complete wetting mode in these cases is further demonstrated in Fig. S5 for spreading 1.25 CMC NaAOTtBC solution on rapeseed oil. Noticeably, the spread area is not circular, but elongated. The deviation from the circular shape was observed also in other cases of small concentrations. This non-circularity can be ascribed to the temperature gradients along the surface of the Petri dish causing also movement of small lenses. Effect of thermal gradients is noticeable only for the cases of slow spreading, when the spreading rate is lower or comparable to the rate of movement due to thermal gradients.

3.3. Fast spreading of ionic surfactant solutions with large spreading coefficients

3.3.1. Sodium surfactants

An increase in surfactant concentration and in dynamic spreading coefficient for Na surfactants to $S > 4$ mN/m resulted in transition to rapid spreading, with characteristic spreading time decreasing up to 2 orders of magnitude as shown in Fig. 6 for NaAOTtBC and in Fig S6 for NaAOTSiC. The maximum spreading rate for these surfactants varies from 355 mm^2/s for 2.5 CMC NaAOTSiC on mineral oil to 3660 mm^2/s for 20 CMC NaAOTSiC on mineral oil, i.e. is 2–3 orders of magnitude larger than for slow spreading. The spread area in Fig. 6 increases nearly linearly with time and spreading exponents (shown in Fig. 6) found from the graphs in log/log coordinates are close to 1, considerably larger than those for silicone oil spreading on glycerol/water substrate. Comparison of results between Fig. 6 and Fig. 4 shows that despite the larger spreading exponent, the spread area on time scale $t \leq 3$ s is smaller for NaAOTtBC solution at small concentration 2.5 CMC than that of pure liquid. This can be related to much smaller spreading coefficients for these solutions, as the spread area is proportional to spreading coefficient (Eqs. (6) and (7)). For all higher concentrations, surfactant solutions spread faster than pure liquid on the substrate of the same viscosity. The difference becomes especially pronounced at high surfactant concentrations.

The exponents are smaller than predicted by Eq. (7) for monolayer spreading over a deep liquid substrate, but are in good agreement with Eq. (6) for thin liquid substrate as well as with spreading rates for surfactant solutions found in [41] for spreading of aqueous solutions of trisiloxane surfactants over thin (4 mm height) mineral oil substrate. Direct calculations using Eq. (6) predict for spread area on mineral oil 1200 and 1100 mm^2 for concentration 20 and 10 CMC respectively for spreading time $t = 0.68$ s taking $K_1 = 1$. This is in good agreement with experimental data (1310 and 1130 mm^2) especially considering the slightly larger spreading exponents found. However, for a concentration of 5 CMC, Eq. (6) predicts a spread area of 840 mm^2 at $t = 0.68$ s, whereas the real spreading area is less than half this value, 376 mm^2. This together with data for concentration of 2.5 CMC confirms that spreading can be slowed down at smaller surfactant concentrations where surfactant mass transfer and adsorption kinetics are the limiting parameters for spreading kinetics. Such an effect was observed earlier for the fast spreading of solutions of surfactants soluble in substrate phase [36], but here the surfactant kinetics limited spreading was also observed for surfactants insoluble in substrate phase. Dependence of spreading kinetics on surfactant concentration was observed for solutions of ionic surfactant dimethyldidodecylammonim bromide (DDAB) in [33], but spreading observed in [33] was rather slow, with maximum spreading rate more than 1 order of magnitude smaller than in the present study.

Performing the same calculations for spreading on rapeseed oil, the spread area can be matched to experimental data for concentration 10 CMC using $K_1 = 1.65$. With this value of K_1, the calculated spread areas for two smaller concentrations are in good agreement if dynamic spreading coefficients are used. The reason for such considerable difference in K_1 for two substrates is not clear. Although such dependence on substrate was observed earlier [39], but it was much smaller than in this study, within 20 %. A possible reason for such difference is the composition of rapeseed oil, which contains free fatty acids being surface active substances. The fatty acids can interact with the studied surfactants changing the composition of adsorbed layers. Measurement at different relative humidities, (RH are given in graph legends in Fig. 6) for both substrates show that a noticeable effect of humidity was observed only for smallest concentration, 2.5 CMC.

For another Na surfactant, NaAOTSiC, Fig. S6, spreading at concentration 2.5 CMC on both substrates is rather slow and in log/log coordinates show three distinct stages, with a short (~0.1 s) induction period, when spreading exponent is in the range 0.6–0.7 followed by a fast spreading ($\alpha > 1$) which slows down on the time scale of 0.5 s. Such spreading kinetics can be explained by smaller CMC value of NaAOTSiC

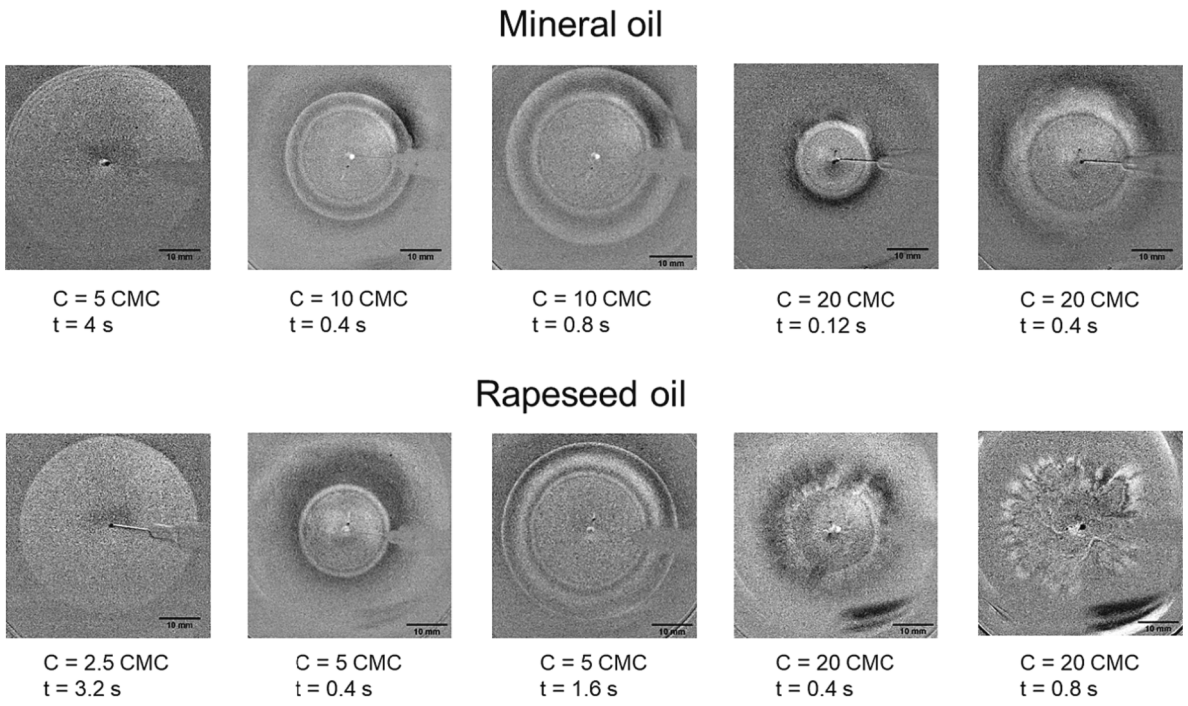

Fig. 7. Typical patterns at spreading of NaAOTtBC solutions.

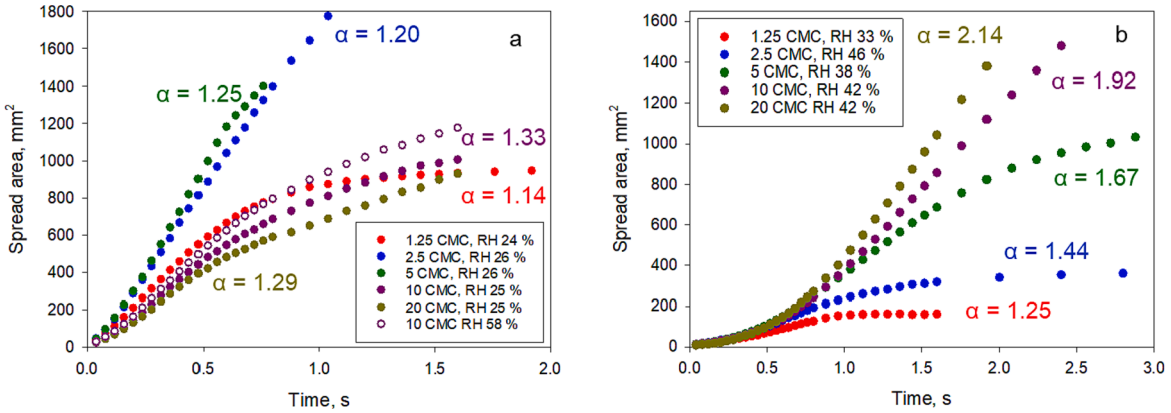

Fig. 8. Spreading kinetics on mineral oil of $Mg(AOTtBC)_2$ (a) and $Mg(AOTSiC)_2$ (b). The spreading coefficients of $Mg(AOTtBC)_2$ solutions (a) are: 1.25 CMC – 7.7/8.2 mN/m, 2.5 CMC – 8.3/8.4 mN/m, 5 CMC – 8.4 mN/m, 10 CMC – 8.3 mN/m, 20 CMC – 8.1 mN/m. The spreading coefficients of $Mg(AOTSiC)_2$ solutions (b) are: 1.25 CMC – 7.8/8.5 mN/m, 2.5 CMC – 9.1/9.3 mN/m, 5 CMC – 9.1/9.3 mN/m, 10 CMC – 9.1/9.3 mN/m, 20 CMC – 9.1/9.3 mN/m.

and its larger molecular mass which can result in slower equilibration (therefore induction period) and faster depletion resulting in earlier slowdown of the spreading. Slower spreading means that it is difficult to support simultaneously a positive spreading coefficient at TPCL and a large enough surface/interfacial tension gradient to support fast spreading. The spread area at the time scale of experiment in Fig. S6 is smaller than that in Fig. 4 for surfactant concentration of 2.5 CMC and larger for all other concentrations similar to NaAOTtBC.

Note, both dynamic and equilibrium spreading coefficients on rapeseed oil are noticeably larger for solution of 2.5 CMC NaAOTSiC than for 2.5 CMC NaAOTtBC, whereas spreading kinetics is considerably slower. At the same time, at higher concentration kinetics of NaAOTSiC is faster in line with larger spreading coefficients. This is one more manifestation of importance of surfactant mass transfer and adsorption kinetics on spreading performance of solution.

The spreading patterns are rather similar for Na surfactants on both substrates. For NaAOTtBC (Fig. 7) the patterns on mineral oil are shifted to the larger concentrations when compared with rapeseed oil. At small concentrations, spreading is homogeneous with a plain circular pattern, whereas a ridge appears at the leading edge of spreading at larger concentrations. The ridge becomes unstable when the concentration grows further. Spreading of 20 CMC NaAOTtBC solution on rapeseed oil demonstrates a pronounced finger instability at the ridge which is so strong that it is impossible to measure the spread area. For NaAOTSiC (Fig. S7), a rather mild ridge instability is noticeable only for spreading of 20 CMC solution on rapeseed oil. For the smallest concentration of NaAOTSiC demonstrating fast spreading, 2.5 CMC, uniform circular patterns are observed at the beginning of spreading. However, when spreading considerably slows down at long spreading times, the patterns become non-circular. As mentioned earlier, such non-uniformity can be due to temperature gradients and thermal Marangoni flows across the substrate.

3.3.2. *Magnesium surfactants*

For the magnesium ionic surfactants spreading coefficients (Table 2, Appendix) are practically independent of concentration and the

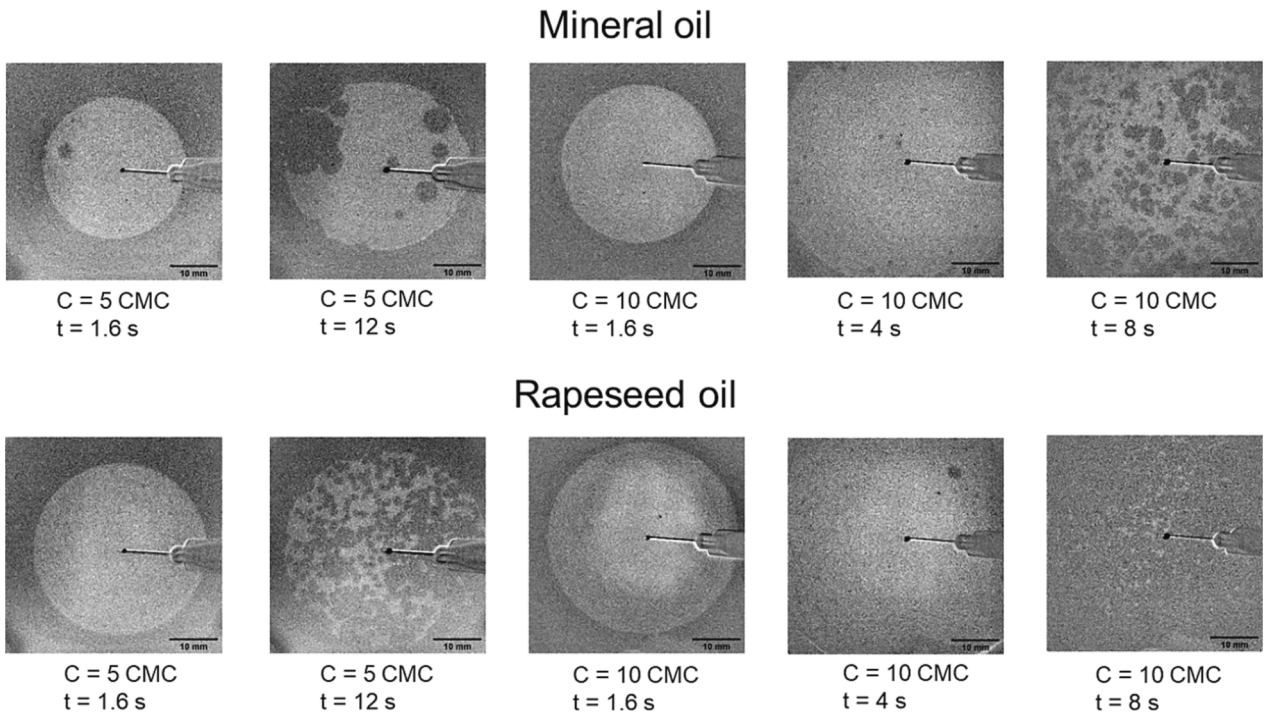

Fig. 9. Typical patterns at spreading of $Mg(AOTSiC)_2$ solutions.

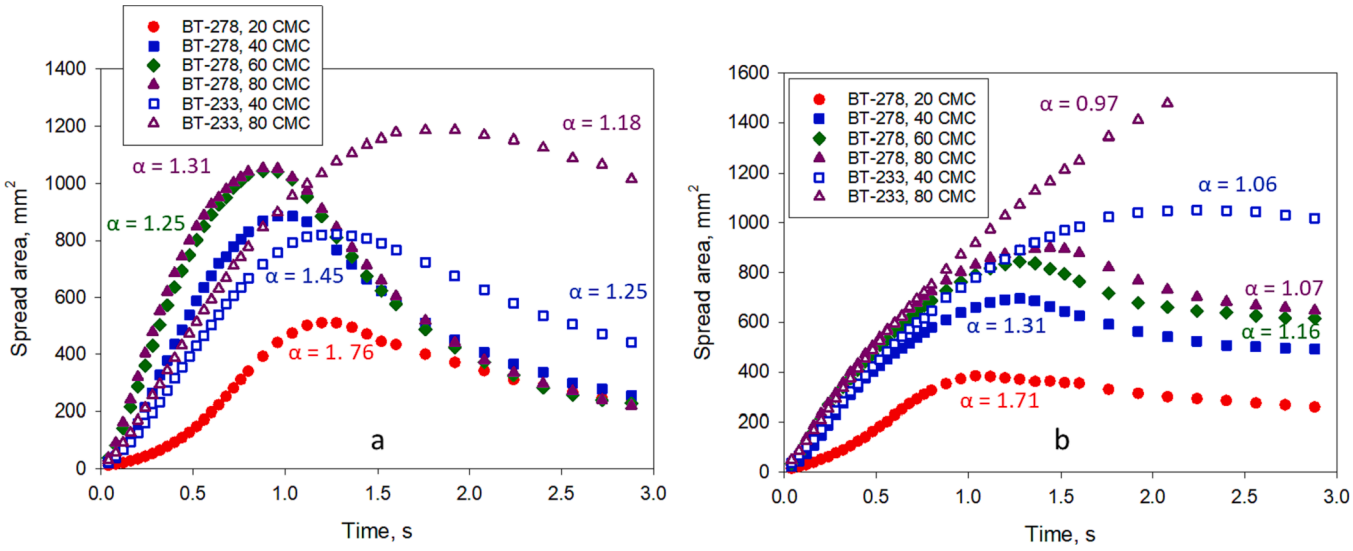

Fig. 10. Spreading kinetics of BT-278 and BT-233 on mineral oil (a) and rapeseed oil (b). The spreading coefficients on mineral oil (a) are: BT-278 40 CMC – 7.6 mN/m, BT-278 80 CMC – 8.3 mN/m, BT-233 40 CMC – 5.5 mN/m, BT-233 80 CMC – 6.0 mN/m. The spreading coefficients on rapeseed oil (b) are: BT-278 40 CMC – 8.8 mN/m, BT-278 80 CMC – 10.2 mN/m, BT-233 40 CMC – 8.2 mN/m, BT-233 80 CMC – 8.7 mN/m.

difference between dynamic and equilibrium spreading coefficients is rather small despite considerably smaller CMC values. Despite the similarity of spreading coefficients, the spreading kinetics are strongly concentration-dependent, demonstrating that surfactant dynamics and mass transfer to the expanding interfaces is more important than the equilibrium values of interfacial tension and spreading coefficients, so long as they are positive and large enough. Dependence of spreading kinetics on concentration also shows that submicron particles, present after filtration of the dispersion through the 1 μm syringe filter, can be equally effective in monomer supply to the depleted solution as self-assembled structures. The spreading kinetics for Mg surfactants on mineral oil is presented in Fig. 8, spreading on rapeseed oil is quite similar. The CMC value of $Mg(AOTSiC)_2$ is 4 times smaller than of Mg $(AOTtBC)_2$ assuming much slower mass transfer for this surfactant. Indeed spreading of $Mg(AOTSiC)_2$ is characterised by a much longer induction stage of slow spreading and for small concentrations, 1.25 and 2.5 CMC, spreading slows down after a short time. The smallest spreading rate during the fast stage observed for solution of 1.25 CMC of $Mg(AOTSiC)_2$ is around 200 mm^2/s, still 2 orders of magnitude larger than that observed in the slow spreading mode presented in Fig. 5. The stage of fast spreading becomes more prolonged and the spreading exponent for this stage increases as concentration increases. At small concentrations, 1.25 and 2.5 CMC, spreading is slower than spreading of silicone oil, but it becomes faster at larger concentrations.

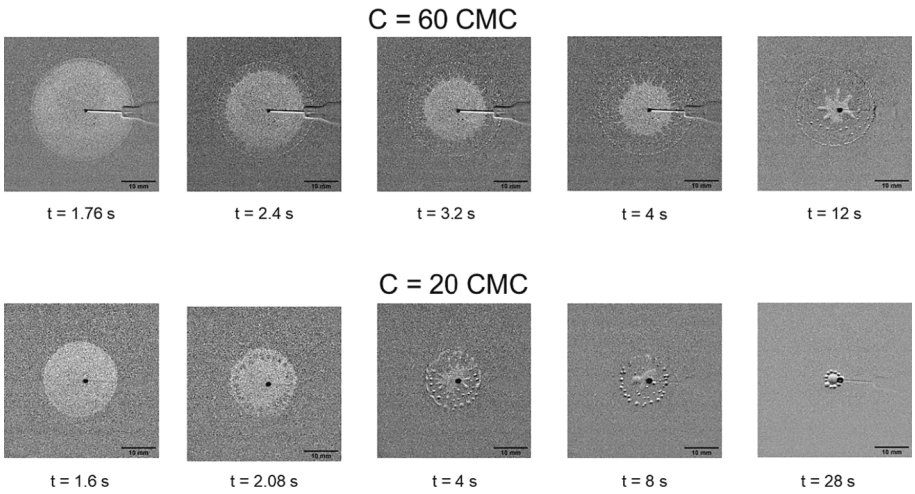

Fig. 11. Instability patterns accompanying dewetting of solutions of BT-278 on rapeseed oil depending on concentrations.

Table 2
Spreading coefficients.

Oil	Oil ST, mN/m	Surfactant	Concentration, CMC	ST, mN/ m	IT, mN/m	Spreading coef. mN/m
Mineral	31.7	NaAOTtBC	1.25	31.3/23.3	8.8/7.4	−8.4/1
Mineral	31.7	NaAOTtBC	2.5	25.7/23.1	4/3.7	2/4.9
Mineral	31.7	NaAOTtBC	5	22.9	2.9	5.9
Mineral	31.7	NaAOTtBC	10	22.3	1.7	7.7
Mineral	31.7	NaAOTtBC	20	22.3	1	8.4
Rapeseed	34.5	NaAOTtBC	1.25	31.3/23.3	7.8/6.1	−4.7/5.1
Rapeseed	34.5	NaAOTtBC	2.5	25.7/23.1	4.4/4	4.4/7.4
Rapeseed	34.5	NaAOTtBC	5	24.5/22.9	3.5/3.2	6.5/8.4
Rapeseed	34.5	NaAOTtBC	10	22.3	2.2	10.0
Rapeseed	34.5	NaAOTtBC	20	22.3	1.5	10.7
Mineral	31.7	Mg(AOTtBC)2	1.25	22.6/22.3	1.4/1.2	7.7/8.2
Mineral	31.7	Mg(AOTtBC)2	2.5	22.2/22.1	1.2	8.3/8.4
Mineral	31.7	Mg(AOTtBC)2	5	22.1	1.2	8.4
Mineral	31.7	Mg(AOTtBC)2	10	22.2	1.2	8.3
Mineral	31.7	Mg(AOTtBC)2	20	22.4	1.2	8.1
Rapeseed	34.5	Mg(AOTtBC)2	1.25	22.6/22.3	1.4/1	7.7/8.4
Rapeseed	34.5	Mg(AOTtBC)2	2.5	22.2/22.1	1.4/1	8.1/8.6
Rapeseed	34.5	Mg(AOTtBC)2	5	22.1	1.4/1	8.2/8.6
Rapeseed	34.5	Mg(AOTtBC)2	10	22.2	1.4/1	8.2/8.6
Rapeseed	34.5	Mg(AOTtBC)2	20	22.4	1.4/1	8.2/8.6
Mineral	31.7	NaAOTSiC	1.25	29.1/22.4	7.2/2.9	−4.6/6.4
Mineral	31.7	NaAOTSiC	2.5	22.3/21.4	3.2/1.3	6.2/9
Mineral	31.7	NaAOTSiC	5	21.4/21.2	1.3/1.2	9/9.3
Mineral	31.7	NaAOTSiC	10	21	1.2	9.5
Mineral	31.7	NaAOTSiC	20	20.9	1.1	9.7
Rapeseed	34.5	NaAOTSiC	1.25	29.1/22.4	7.5/3.9	−2.1/8.2
Rapeseed	34.5	NaAOTSiC	2.5	22.3/21.4	2.1/1.7	10.1/11.4
Rapeseed	34.5	NaAOTSiC	5	21.4/21.2	2.0/1.6	11.1/11.7
Rapeseed	34.5	NaAOTSiC	10	21	1.8/1.6	11.7/11.9
Rapeseed	34.5	NaAOTSiC	20	20.9	1.7/1.5	11.9/12.1
Mineral	31.7	Mg(AOTSiC)2	1.25	21.9/21.4	2/1.8	7.8/8.5
Mineral	31.7	Mg(AOTSiC)2	2.5	21.3/21.2	1.4/1.2	9.1/9.3
Mineral	31.7	Mg(AOTSiC)2	5	21.2/21.1	1.4/1.2	9.1/9.3
Mineral	31.7	Mg(AOTSiC)2	10	21.2/21.1	1.4/1.2	9.1/9.3
Mineral	31.7	Mg(AOTSiC)2	20	21.2/21.1	1.4/1.2	9.1/9.3
Rapeseed	34.5	Mg(AOTSiC)2	1.25	21.9/21.4	2.1/1.1	10.5/12
Rapeseed	34.5	Mg(AOTSiC)2	2.5	21.3/21.2	2.1/1.1	10.5/12
Rapeseed	34.5	Mg(AOTSiC)2	5	21.2/21.1	2.1/1.1	10.5/12
Rapeseed	34.5	Mg(AOTSiC)2	10	21.2/21.1	2.1/1.1	10.5/12
Rapeseed	34.5	Mg(AOTSiC)2	20	21.2/21.1	2.1/1.1	10.5/12
Mineral	31.7	BT-233	40	22.7	3.5	5.5
Mineral	31.7	BT-233	80	22.5	3.2	6.0
Rapeseed	34.5	BT-233	40	22.7	3.6	8.2
Rapeseed	34.5	BT-233	80	22.5	3.3	8.7
Mineral	31.7	BT-278	40	20.7	3.4	7.6
Mineral	31.7	BT-278	80	20.6	2.8	8.3
Rapeseed	34.5	BT-278	40	20.7	5.0	8.8
Rapeseed	34.5	BT-278	80	20.6	3.7	10.2

For $Mg(AOTtBC)_2$ there is practically no induction stage and the spreading slows down at later times at small concentrations. The fastest spreading is observed at concentrations of 2.5 and 5 CMC. It is faster than the spreading of silicone oil. Spreading slows down at higher concentrations. The reason for such concentration dependence can be an unfavourable dependence of Marangoni stresses on concentration. However, the non-monotonous concentration dependence was not observed for any other surfactant studied here, either with larger or smaller CMC. Therefore, it is more probable that this is the effect of increased concentration of submicron particles. The particle concentration in solutions of $Mg(AOTSiC)_2$ is smaller because of its smaller CMC. A similar dependence of spreading performance was observed for $Mg(AOTSiC)_2$ spreading on solid substrate, but at larger concentration of 60 CMC [5]. It was suggested in [4] that spreading of trisiloxane superspreaders on a solid substrate slows down at high concentrations because it is hindered by a high concentration of lamellar phase at the TPCL. The argument in favour of this explanation is a continuous spreading under conditions of high humidity RH = 100 %. Spreading of solutions of $Mg(AOTtBC)_2$ at higher concentrations in this study changes very little by increase of humidity from RH = 25 % to RH = 58 %. Therefore, this phenomenon requires a more thorough future study.

Note, $Mg(AOTSiC)_2$ was proved to be a superspreader on a solid substrate polyvinylidenefluoride [5], while other branched ionic surfactants were not. Spreading results on liquid substrates show that there is no specific difference between spreading of solutions of $Mg(AOTSiC)_2$ and other surfactants which cannot be explained by difference in spreading coefficients and adsorption kinetics.

Spreading patterns for Mg surfactants (Fig. 9 and Fig. S8) are rather different from what was observed for Na surfactants. In particular, no ridge was observed over the whole studied range of concentrations. Instead, after a certain time of spreading, black holes started to nucleate inside the spread area. With time these holes have grown while new holes were nucleated and the area occupied by holes increased with time until all visible parts of spread film disappeared. From the presented set of experiments, it is impossible to conclude whether these black holes show the clean subphase interface or if they are invisible thin films (black films) stabilised by surfactant. The role of particles present in the spreading Mg solutions on holes nucleation is also unclear. Therefore, a further study is under way to address these questions.

3.4. Spreading of non-ionic surfactant solutions

The non-ionic surfactants used in this study are soluble in both oil phases. As a consequence, much higher surfactant concentrations are necessary to achieve high spreading rates on a liquid substrate compared with a solid substrate. For spreading on a solid hydrophobic substrate, the optimal concentration of BT-278 providing the maximum spread area is around 10 CMC [27], whereas for spreading on oil the spread area reaches a maximum at a concentration of 80 CMC (see Fig. 10). The spread area increases rapidly after drop deposition, but then begins to decrease. The reason for this is surfactant depletion at the leading edge of spreading due to adsorption on expanding liquid/air and liquid/substrate interface and due to dissolution into substrate phase. When the concentration at the TPCL decreases so much that the spreading coefficient becomes negative, spreading stops and dewetting begins. The time till the reversal is shorter for spreading on mineral oil than on rapeseed oil. Spread area decreases more slowly on rapeseed oil than on mineral oil and for BT-233 slower than for BT-278, supposedly due to a decrease of surfactant solubility in the oil phase.

The induction time before the onset of fast spreading is well visible, especially for the smallest concentration BT-278, Fig. 10. Values of spreading exponents for fast spreading stage at concentrations 60 and 80 CMC are close to 1 as expected for the spreading on thin liquid substrate. Surprisingly, the spreading exponents increase with a decrease in concentration and the corresponding decrease in the spreading rate and are closer to 1.5 characteristic for spreading on a deep layer at concentration 40 CMC. This indicates that the spreading exponent does not completely characterise the spreading process and the pre-exponential coefficient can be even more important, especially for surfactants soluble in the substrate phase. Similar to branched ionic surfactants, there is no noticeable qualitative difference in the spreading of surfactants demonstrating superspreading (BT-278) and non-superspreading (BT-233) behaviour on solid.

BT-233 spreads on both substrates forming uniform circular patterns without a ridge at the leading edge of spreading, see Fig. S9. When the spread area decreases, it remains circular with some random deviations from circularity at $t > 4$ s. The spreading of BT-278 follows the same plain circular pattern, but dewetting patterns are different from BT-233. Dewetting on mineral oil is accompanied by weak instability near TPCL, which sometimes results in nucleation and growth of 1 or 2 nearly circular indents on the spread film (see Fig. S9). On rapeseed oil, instability results in formation sophisticated patterns shown in Fig. 11. The wavelength of the pattern decreases with an increase of surfactant concentration.

This instability pattern looks very similar to one described in [52], which resulted from spreading of mixture of water and a volatile alcohol on sunflower oil. Similarly to the spreading of BT-278 solution, the instability wavelength in [52] decreased with an increase in alcohol concentration. According to [52] instability is induced by alcohol evaporation. As the thickness of spreading drop is smaller near TPCL, the evaporation causes much larger increase in surface/interfacial tension here than close to the drop centre. As a result, the spreading coefficient at the TPCL can become negative and simultaneously large concentration gradients are formed between the central part of the drop and periphery, resulting in flow directed towards the TPCL. These factors lead to formation of a thick ridge which splits into drops due to a mechanism similar to Plateau-Rayleigh instability. In the case presented in Fig. 11, instability is caused not by evaporation but by dissolution of the surface-active component of the solution. It is interesting that in both, this study and [52], this kind of instability was observed by spreading of aqueous solution on vegetable oil. This raises the question about the possible role of free fatty acids present in these oils in the instability development.

4. Conclusions

This study has shown that all probed branched ionic surfactants have positive equilibrium spreading coefficients and demonstrate very fast spreading (superspreading) on the liquid oil substrates employed. Similar fast spreading on oil was reported in the literature so far only for fluorocarbon ionic surfactants [39]. Hydrocarbon ionic surfactant, dimethyldidodecylammonim bromide (DDAB) demonstrated complete wetting on oil substrates, but observed spreading kinetics was noticeably slower [33]. Another study [41] reported that DDAB does not demonstrate surfactant-enhanced spreading on mineral oil, although surfactant concentration and corresponding spreading coefficient were not mentioned in this study.

If the equilibrium spreading coefficient of surfactant solution is positive, spreading can occur in two difference modes depending on dynamic spreading coefficient. If dynamic spreading coefficient on time scale of drop formation and deposition is negative, or positive but rather small (below 4 mN/m in this study) spreading is slow, with characteristic time scale of spreading being in the range of minutes. The maximum observed spreading rate in this regime was below 1.4 mm^2/s. If dynamic spreading coefficient was above 4 mN/m, fast spreading with characteristic timescale in the range of seconds developed. The maximum spreading rate in this regime exceeded 200 mm^2/s. Slow regime of complete wetting for surfactants demonstrating superspreading at higher concentrations was not reported in the previous studies. The study has shown that although complete wetting requires only a non-negative spreading coefficient, fast spreading requires the spreading coefficient to be considerably greater than zero.

The slow spreading of surfactant solutions is much slower than spreading of pure liquid (silicone oil) on substrates of the same depth

and viscosity. For the fast spreading, spreading exponents are considerably larger than those found for spreading of pure liquid, but at small surfactant concentrations (typically 1.25 and 2.5 CMC) kinetics is slower. Slower induction stage, early retardation of spreading and smaller pre-exponential factor all contribute to this difference. All this is indication of adsorption governed spreading kinetics, suggested as a limiting step for spreading of aqueous surfactant solutions on liquid oil substrates in [33,36]. For one of the surfactants, $Mg(AOTtBC)_2$, spreading was slowing down at concentrations 10 and 20 CMC, supposedly due to effect of large concentration of submicron particles present. For this surfactant spreading at concentrations 2.5 and 5 CMC was faster than the spreading of silicone oil. A maximum of spreading rate dependence on concentration is typical for spreading on solid substrate [2,27] The dependence of Marangoni stresses on liquid surface on surfactant concentration [3] and an increase of the liquid viscosity close to TPCL due to increase concentration of surfactant aggregates [4] were named as a possible reason of this concentration dependence. The range of surfactant concentrations enabling superspreading on solid surface was found to be dependent of the intensity of direct transfer (leakage) of surfactant through the TPCL in [20]. As this is the first time such an effect was observed for spreading on a liquid substrate, a more thorough investigation is required to provide an explanation.

For non-ionic surfactants soluble in oil, spreading area reached maximum and then started to decrease, because surfactant dissolution resulted in decrease of spreading coefficient to negative values. Such a behaviour was observed earlier for spreading non-ionic trisiloxane surfactants on deep oil substrates [36]. The spreading exponents and the spreading rates during the spreading stage were in line with those for ionic surfactants not soluble in oil. The optimal surfactant concentrations enabling the fastest spreading on oil are much higher than reported for spreading the same surfactant solutions on solid substrate [27].

There was no difference in the spreading behaviour between surfactants proved to be superspreaders on solid substrate and non-superspreaders. This is the first time such a comparison has been made taking into account the spreading coefficients. The only study mentioning comparison of superspreading and non-superspreading surfactants performance on oil substrate [41] found that behaviour was similar on solid and liquid substrates. However, this study did not report spreading coefficients involved and the authors suggested that probably the condition of complete wetting, $S > 0$ was not met for non-superspreading surfactants in their study.

Spreading and dewetting resulted in a number of spreading patterns including uniform circular spreading, formation of a ridge at the leading edge of spreading, fingering instability at the ridge, nucleation and growth of black spots within the spreading area, formation of series of drops at dewetting. The last pattern was observed for the spreading on rapeseed oil of a surfactant soluble in this oil. A similar pattern was observed in [52] for spreading of water/alcohol mixture on sunflower oil. While the effect of surfactant transfer/loss, due to evaporation [52] and dissolution in oil in this study is unquestionable for this phenomenon, the role of substrate, which was a vegetable oil having free fatty acids in its composition in both cases is unclear and requires an additional study.

CRediT authorship contribution statement

Nina M. Kovalchuk: Conceptualization, Formal analysis, Investigation, Methodology, Writing – original draft, Visualization. **Masanobu Sagisaka:** Conceptualization, Funding acquisition, Methodology, Supervision, Writing – review & editing. **Hinata Komiyama:** Investigation, Visualization. **Mark J.H. Simmons:** Conceptualization, Funding acquisition, Resources, Writing – review & editing.

Declaration of competing interest

The authors declare that they have no known competing financial interests or personal relationships that could have appeared to influence the work reported in this paper.

Data availability

No data was used for the research described in the article.

Acknowledgments

This research was funded by The Royal Society, UK and JSPS, Japan, through International Exchanges 2021 Cost Share (JSPS) award 1845272; EPSRC, UK, through the PREMIERE Programme Grant EP/T000414/1 and KAKEN HI Grant-in-Aid for Scientific Research (B) 19H02504. We also acknowledge Dr Sarah Rogers for supporting SANS experiment and STFC for the allocation of beam time at ISIS and Dr Joachim Venzmer (Evonic) for donating trisiloxane surfactants for this study.

Appendix A

Appendix B. Supplementary data

Supplementary data to this article can be found online at https://doi.org/10.1016/j.jcis.2024.02.031.

References

[1] N.M. Kovalchuk, M.J.H. Simmons, Surfactant-mediated wetting and spreading: Recent advances and applications, Curr. Opin. Colloid Interface Sci. (2021) 51.
[2] R.M. Hill, Superspreading, Curr. Opin. Colloid Interface Sci. 3 (1998) 247–254.
[3] A. Nikolov, D. Wasan, Current opinion in superspreading mechanisms, Adv Colloid Interface Sci. 222 (2015) 517–529.
[4] J. Venzmer, Superspreading - Has the mystery been unraveled? Adv Colloid Interface Sci. 288 (2021) 102343.
[5] N.M. Kovalchuk, M. Sagisaka, S. Osaki, M.J.H. Simmons, Superspreading performance of branched ionic trimethylsilyl surfactant Mg(AOTSiC)2, Colloids Surfaces A: Physicochem. Eng. Aspects (2020) 604.
[6] N.M. Kovalchuk, A. Barton, A. Trybala, V. Starov, Mixtures of catanionic surfactants can be superspreaders: Comparison with trisiloxane superspreader, J Colloid Interface Sci. 459 (2015) 250–256.
[7] P.G. de Gennes, F. Brochard-Wyart, D. Quere, Capillarity and wetting phenomena. Drops, bubbles, pearls, waves, Springer, New York, 2004.
[8] D. Li, A.W. Neumann, Equation of state for interfacial tension of solid-liquid systems, Adv Colloid Interface Sci. 39 (1992) 299–345.
[9] E. Chibowski, Some problems of characterization of a solid surface via the surface free energy changes, Adsorpt. Sci. Technol. 35 (2017) 647–659.
[10] D. Mańko, A. Zdziennicka, J. Krawczyk, B. Jańczuk, Wettability prediction of such polymers as polyethylene and polytetrafluoroethylene by aqueous solutions of classical surfactants and biosurfactants, Colloids Surfaces A: Physicochem. Eng. Aspects 506 (2016) 409–415.
[11] G. Whyman, E. Bormashenko, T. Stein, The rigorous derivation of Young, Cassie-Baxter and Wenzel equations and the analysis of the contact angle hysteresis phenomenon, Chem. Phys. Lett. 450 (2008) 355–359.
[12] H.Y. Erbil, C.E. Cansoy, Range of applicability of the Wenzel and Cassie-Baxter equations for superhydrophobic surfaces, Langmuir. 25 (2009) 14135–14145.
[13] P.D. Ravazzoli, A.G. González, J.A. Diez, H.A. Stone, Buoyancy and capillary effects on floating liquid lenses, Phys. Rev. Fluids. (2020) 5.
[14] A. Nepomnyashchy, Droplet on a liquid substrate: Wetting, dewetting, dynamics, instabilities, Curr. Opin. Colloid Interface Sci. 51 (2021).
[15] D. Vollhardt, V.B. Fainerman, Characterisation of phase transition in adsorbed monolayers at the air/water interface, Adv Colloid Interface Sci. 154 (2010) 1–19.
[16] S. Manne, H.E. Gaub, Molecular Organization of Surfactants at Solid-Liquid Interfaces, Science. 270 (1995) 1480–1482.
[17] R. Saino, M. Akamatsu, K. Sakai, H. Sakai, Morphology of surfactant mixtures at solid/liquid interfaces: High-speed AFM observation, Colloids Surfaces A: Physicochem. Eng. Aspects (2021) 616.
[18] T. Svitova, R.M. Hill, C.J. Radke, Adsorption layer structures and spreading behavior of aqueous non-ionic surfactants on graphite, Colloids Surfaces A: Physicochem. Eng. Aspects 183–185 (2001) 607–620.
[19] G. Karapetsas, R.V. Craster, O.K. Matar, On surfactant-enhanced spreading and superspreading of liquid drops on solid surfaces, J. Fluid Mech. 670 (2011) 5–37.
[20] H.-H. Wei, Marangoni-enhanced capillary wetting in surfactant-driven superspreading, J. Fluid Mech. 855 (2018) 181–209.
[21] G. Karapetsas, R.V. Craster, O.K. Matar, Surfactant-driven dynamics of liquid lenses, Phys. Fluids. 23 (2011).

[22] L. Tanner, The spreading of silicone oil drops on horisontal surfaces, J. Phys. D: Appl. Phys. 12 (1979) 1473–1484.
[23] J.G.E.M. Fraaije, A.M. Cazabat, Dynamics of spreading on a liquid substrate, J. Colloid Interface Sci. 133 (1989) 452–460.
[24] B.M. Marino, L.P. Thomas, J.A. Diez, R. Gratton, Capillarity effects on viscous gravity spreadings of wetting liquids, J. Colloid Interface Sci. 177 (1996) 14–30.
[25] H.E. Huppert, The propagation of two-dimensional and axisymmetric viscous gravity currents over a rigid horizontal surface, J. Fluid Mech. 121 (2006).
[26] R. Gratton, J.A. Diez, L.P. Thomas, B. Marino, S. Betelu, Quasi-self-similarity for wetting drops, Phys. Rev. E Stat. Phys. Plasmas Fluids Relat. Interdiscip. Topics. 53 (1996) 3563–3572.
[27] N.M. Kovalchuk, J. Dunn, J. Davies, M.J.H. Simmons, Superspreading on hydrophobic substrates: effect of glycerol additive, Colloids Interfaces (2019) 3.
[28] E. Ruckenstein, Superspreading: A possible mechanism, Colloids Surfaces A: Physicochem. Eng. Aspects 412 (2012) 36–37.
[29] F. Tiberg, A.M. Cazabat, Self-assembly and spreading of non-ionic trisiloxane surfactants, Europhys. Lett. 25 (1994) 205–210.
[30] J. Ahmad, R.S. Hansen, A simple quantitative treatment of the spreading of monolayers on thin liquid films, J Colloid Interface Sci. 38 (1972) 601–604.
[31] P. Joos, J. Pintens, Spreading kinetics of liquids on liquids, J. Colloid. Interface Sci. 60 (1977) 507–513.
[32] V. Bergeron, D. Langevin, Monolayer spreading of polydimethylsiloxane oil on surfactant solutions, Phys Rev Lett. 76 (1996) 3152–3155.
[33] T.F. Svitova, R.M. Hill, C.J. Radke, Spreading of aqueous dimethyldidodecylammonium bromide surfactant droplets over liquid hydrocarbon substrates, Langmuir. 15 (1999) 7392–7402.
[34] F. Brochard-Wyard, G. Debregeas, P.G. de Gennes, Spreading of viscous droplets on a non viscous liquid, Colloid Polymer Sci. 274 (1996) 70–72.
[35] Y.C. Liao, Y.C. Li, H.H. Wei, Drastic changes in interfacial hydrodynamics due to wall slippage: slip-intensified film thinning, drop spreading, and capillary instability, Phys. Rev. Lett. 111 (2013) 136001.
[36] T.F. Svitova, R.M. Hill, C.J. Radke, Spreading of aqueous trisiloxane surfactant solutions over liquid hydrophobic substrates, Langmuir. 17 (2001) 335–348.
[37] P. Joos, J. Van Hunsel, Spreading of aqueous surfactant solutions on organic liquids, J Colloid Interface Sci. 106 (1989) 161–167.
[38] X. Jia, Y. Luo, R. Huang, H. Bo, Q. Liu, X. Zhu, Spreading kinetics of fluorocarbon surfactants on several liquid fuels surfaces, Colloids Surfaces A: Physicochem. Eng. Aspects (2020) 589.
[39] X. Jia, Y. Luo, R. Huang, X. Zhu, Y. Zhang, Q. Liu, Two-dimensional spreading properties and sealing characteristics of fluorocarbon surfactants on several typical hydrocarbon fuels, Sci. Rep. 11 (2021) 1148.
[40] Y. Sheng, Y. Li, W. Ma, H. Zhang, Spreading behavior of firefighting foam solutions on typical liquid fuel surfaces, J. Surfactants Detergents. 25 (2022) 789–798.
[41] T. Stoebe, Z. Lin, R.M. Hill, M.D. Ward, H.T. Davis, Superspreading of aqueous films containing trisiloxane surfactant on mineral oil, Langmuir. 13 (1997) 7282–7286.
[42] V. Starov, Static contact angle hysteresis on smooth, homogeneous solid substrates, Colloid Polymer Sci. 291 (2013) 261–270.
[43] A. Czajka, C. Hill, J. Peach, J.C. Pegg, I. Grillo, F. Guittard, et al., Trimethylsilyl hedgehogs - a novel class of super-efficient hydrocarbon surfactants, Phys. Chem. Chem. Phys. 19 (2017) 23869–23877.
[44] N.M. Kovalchuk, E. Nowak, M.J.H. Simmons, Kinetics of liquid bridges and formation of satellite droplets: Difference between micellar and bi-layer forming solutions, Colloids Surfaces A: Physicochem. Eng. Aspects 521 (2017) 193–203.
[45] J. Venzmer, S.P. Wilkowski, Trisiloxane surfactants – mechanisms of spreading and wetting, in: J.D. Nalewaja, G.R. Goss, R.S. Tann (Eds.), Pesticide Formulations and Application Systems: Am. Soc. For Testing and Materials, 2016.
[46] G.P. Association, Physical Properties of Glycerine and Its Solutions New York, Glycerine Producers' Association, USA, 1963.
[47] C.M. Phan, Stability of a floating water droplet on an oil surface, Langmuir 30 (2014) 768–773.
[48] C.A. Schneider, W.S. Rasband, K.W. Eliceiri, NIH Image to ImageJ: 25 years of image analysis, Nat. Methods 9 (2012) 671–675.
[49] M. Sagisaka, T. Endo, K. Fujita, Y. Umetsu, S. Osaki, T. Narumi, et al., Very low surface tensions with "Hedgehog" surfactants, Colloids Surfaces A: Physicochem. Eng. Aspects (2021) 631.
[50] S. Semenov, A. Trybala, R.G. Rubio, N. Kovalchuk, V. Starov, M.G. Velarde, Simultaneous spreading and evaporation: recent developments, Adv Colloid Interface Sci. 206 (2014) 382–398.
[51] D. Exerowa, A. Nikolov, M. Zacharieva, Common Black and Newton Film Formation, J Colloid Interface Sci. 81 (1981) 419–429.
[52] L. Keiser, H. Bense, P. Colinet, J. Bico, E. Reyssat, Marangoni Bursting: Evaporation-Induced Emulsification of Binary Mixtures on a Liquid Layer, Phys Rev Lett. 118 (2017) 074504.